JOURNAL OF MATERIALS SCIENCE 32 (1997) 4767–4775

Fracture toughness of multiphase polypropylene composites containing rubbery and particulate inclusions

P. R. HORNSBY
Department of Materials Engineering, Brunel University, Uxbridge, Middlesex, UK
K. PREMPHET
Department of Chemistry, Mahidol University, Rama VI, Bangkok, Thailand

The fracture toughness of binary and ternary phase polypropylene (PP) composites containing ethylene–propylene rubber (EPR) and glass beads, has been studied using the *J*-integral method at 23 and −20 °C. For determining J_c, analysis of the stress-whitening zone was found to be more meaningful than the commonly used blunting line approach. Functionalized EPR was found to be more effective toughening additive for PP than EPR, in both binary and ternary phase compositions. Crack growth mechanisms were examined by scanning electron microscopy. In rubber-modified blends, cavitation and shear yielding were found to be the primary toughening mechanisms, while in ternary phase composites particle–matrix debonding played a major role.

1. Introduction

Criteria influencing the fracture toughness of polymeric materials have been extensively investigated. One of the most widely adopted methods involves the *J*-integral concept, proposed by Rice [1] and standardized by the ASTM [2] for metallic materials. The aim of this procedure is to determine the *J* integral value for crack initiation, providing a measure of the energy required to create new surfaces. However, to determine this parameter in tough materials, a graphical approach, called "the blunting line concept", is employed, utilizing the following expression

$$J = 2\sigma_y \Delta a \quad (1)$$

where σ_y is the yield stress, and Δa the incremental growth in crack length. In this method, the crack tip is assumed to be blunted with a semicircular geometry prior to initiation. The crack initiation energy, J_c, is the value of *J* at intersection of the crack blunting line and the resistance, *R*, curve, as shown in Fig. 1. This technique has been used to describe toughness criteria in many ductile or impact-resistant polymers, including polypropylene [3, 4], polypropylene copolymer [4–6], polyethylene [4–7], acrylonitrile–butadiene–styrene (ABS) [5, 8], polyamide [5, 6], toughened polyamide [9], modified polycarbonate [10, 11] and polypropylene blends [12]. However, the procedure is involved, causing the validity of the approach to be questioned. For example, Narisawa [4] encountered difficulty in obtaining values of J_c for polyethylene and polypropylene, because with both of these materials, crack blunting was not observed. In studies using ABS, Zhang *et al.* measured the lengths of both the whitening zone and crack growth zone for determination of J_c [8]. Values obtained by these two techniques were in good agreement.

The present work considered the measurement of J_c for multiphase polypropylene composites containing ethylene–propylene rubber and glass beads. The primary objectives of the investigation were to analyse fracture toughness behaviour of these materials by comparing the conventional crack blunting line and the stress-whitening zone techniques and to study the resultant failure mechanism through microstructural observation.

2. Experimental procedure

2.1. Materials

Composites were prepared from polypropylene homopolymer (PP) (Novolen 1100HX (BASF)), with a melt flow rate of 1.8 g/10 min (230 °C/2.16 kg), together with two grades of ethylene–propylene rubber (EPR), namely Exxelor PE808 (Exxon Chemical), which is a semicrystalline grade with melt flow rate of 3 g/10 min (230 °C/10 kg), and a functionalized variant (MaR), Exxelor VA1803 (Exxon Chemical), which is an amorphous maleic–anhydride grafted elastomer with a melt flow rate of 22 g/10 min (230 °C/10 kg). Ternary phase compositions also contained untreated glass beads (G) (Spheriglass 5000, Croxton and Garry Ltd), with median particle diameter in the range of 3.5–7.0 μm.

2.2. Compound and sample preparation

All composites were melt-mixed in a co-rotating twin screw extruder (BTS-40 Betol Machinery Ltd) using

0022–2461

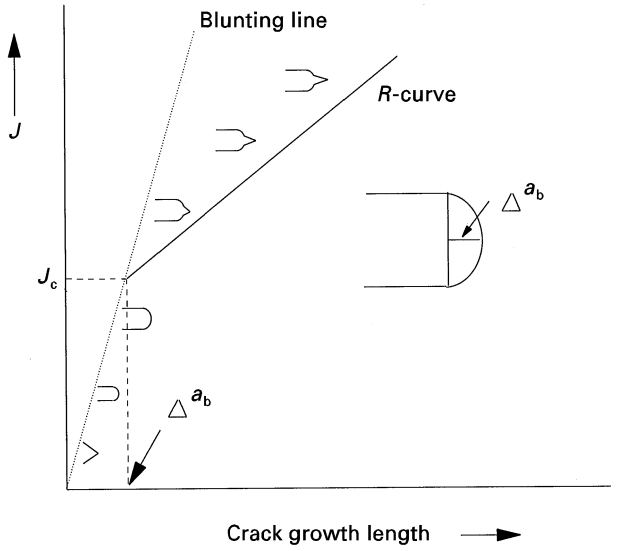

Figure 1 Schematic representation of the *R*-curve and the crack tip blunting component of crack growth.

a single-pass compounding regime. The barrel temperature profile was set between 185 and 200 °C (from feed zone to die). The screw speed used was 170 r.p.m., giving a throughput rate of 20 kg h^{-1}. The composite formulation was kept constant at 70/30 vol % (PP/EPR or MaR) for binary phase elastomer-modified systems, and 70/15/15 vol % (PP/G/EPR or MaR) for ternary phase elastomer-modified polypropylene compositions, containing both glass filler and rubber.

In order to mininize further microstructural changes which might be induced during secondary processing, test specimens for *J* integral measurements were prepared by compression moulding, using a sheet mould with dimensions of 170 mm × 200 mm × 12 mm thick. Great care was taken during processing to ensure that material was fully melted and consolidated and that mouldings produced were defect free. Rectangular bars (24 mm × 108 mm × 12 mm) were cut from the compression-moulded sheet. Details of specimen geometry are shown in Fig. 2. A single-edge 13 mm deep groove was introduced using a saw, then notched with a fresh razor blade. This was discarded after every four samples to ensure consistency in the size and sharpness of the crack. The initial notch depth formed by the saw and razor blade was then measured under a microscope using a micrometer eyepiece. This procedure was in accordance with the ASTM standard which recommends the following specimen geometry in order to achieve plane strain conditions at the crack tip

$$B, a, (W - a) \geqslant 25(J_c/\sigma_y) \quad (2)$$

where σ_y is the tensile yield stress, measured according to the ASTM D638 under the same test conditions as for the *J*-integral test. *B* and *W* are the specimen width and thickness, respectively, and *a* is the initial notch length to the end of the preformed crack.

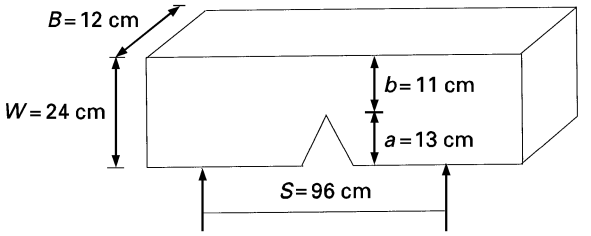

Figure 2 Specimen configuration for the *J*-integral test.

2.3. *J*-integral test procedure

This was undertaken according to ASTM E813-81 [2] at ambient (23 °C) and low (−20 °C) temperatures. Testing was performed in a three-point bending mode, using an Instron tensometer (Model 1195), at a strain rate of 1 mm min^{-1} using a specimen span length of 96 mm. During testing, a series of identical specimens were loaded and unloaded to different predetermined deflections, less than that required to give complete failure. At each deflection, the load–displacement curve was recorded and the energy absorbed up to this point calculated from the area under the curve. The extent of crack growth was obtained using an optical microscope. In samples where the crack was very small or consisted of multiple microcracks, the region of stress-whitening observed was measured instead. Fracture surfaces for determination of the stress-whitening length were prepared by immersing the specimens in liquid nitrogen before breaking in the tensometer. The extent of stress-whitening was measured at the longest part of the whitening zone. The *J*-integral value was subsequently calculated from the following expression

$$J = 2U/B(W - a) \quad (3)$$

where *U* is the input energy to the specimen given by the area under the load–displacement curve. Calculated values for *J* were then plotted against developed crack length to obtain an *R*-curve. Using this method, the *J* value at the onset of crack growth, J_c, was determined at the point of intersection of the *R*-curve and the blunting line, calculated using Equation 1.

In the stress-whitening method, calculated values for *J* were plotted against stress-whitening length (instead of crack growth length), and an *R*-curve obtained comprising two lines of different slope. J_c was determined from their point of intersection.

2.4. Microscopy

In order to elucidate the mechanism of failure in the composites, fracture surfaces were examined using scanning electron microscopy (SEM). These were prepared by immersing test specimens in liquid nitrogen, before breaking them using an Instron testing machine operating at a crosshead speed of 50 mm min^{-1}. Fracture surfaces prepared in this way, were gold-coated then examined in a Cambridge S250 scanning electron microscope.

3. Results and discussion

3.1. Toughness measurements using the conventional blunting line method

Typical load/displacement curves obtained at 23 °C for neat polypropylene (PP) and modified polypropylene containing EPR (PP/R), are shown in Fig. 3. Both curves exhibited the deviation from linearity observed previously by other authors [4, 13]. The relationships between J and crack growth length for these materials are shown in Figs 4 and 5, respectively. Surprisingly, the J_c value for PP/EPR (1.86 kJ m^{-2}) was found to be lower than that for unmodified PP (2.27 kJ m^{-2}) even though the load/displacement curves clearly indicated that the elastomer-modified PP was tougher. A similar observation was recently reported by Ha *et al.* [12] in which the J_c value of a PP/EPDM (50/50) blend was also found to be less than that for neat PP. In the last mentioned study, a locus line method, developed by Kim and Joe [13–15] was used. In the present investigation, the fracture toughness of PP/EPR determined from this conventional blunting line approach is clearly an underestimate.

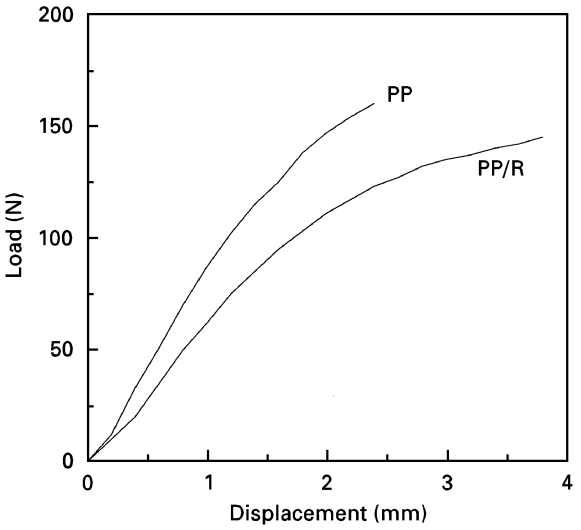

Figure 3 Typical load–displacement curves of PP and PP/EPR at 23 °C.

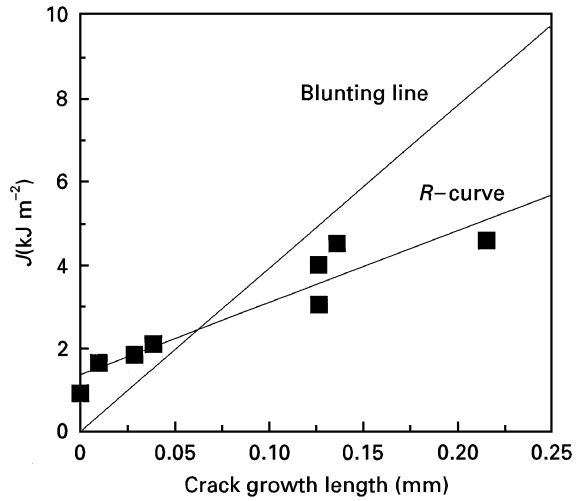

Figure 4 Plot of J against crack growth length for PP at 23 °C.

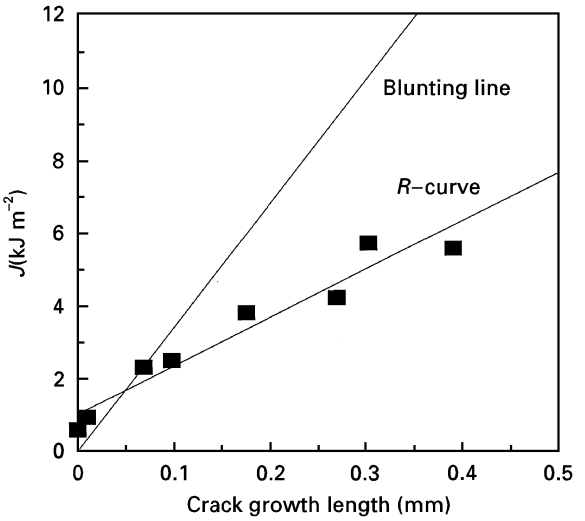

Figure 5 Plot of J against crack growth length for PP/EPR at 23 °C.

J-integral testing was also undertaken at −20 °C, i.e. below the glass transition temperature of PP, where the yield stress of this polymer is increased and plane strain conditions are more fully realized. Plots of J against crack growth length for PP and PP/EPR obtained under these conditions are shown in Figs 6 and 7 giving J_c values of 1.75 and 3.48 kJ m^{-2} for PP and PP/EPR, respectively, and clearly demonstrating the toughening effect of the rubber modifier, under these test conditions.

Greater difficulty was encountered in determining crack growth lengths for ternary phase PP composites, combining elastomer and glass beads. Fig. 8a and b show optical micrographs of PP/G/EPR obtained after testing at −20 °C. Fig. 8a demonstrates that subcritical crack growth is initiated and propagated ahead of the precrack tip, and on increased loading (Fig. 8b), this multiple crack pattern develops further. With neat PP, however, the crack occurring ahead of the precrack tip remains very sharp (Fig. 8c), facilitating measurement of crack growth length.

Hence, there are several reasons why the crack blunting line concept is not suitable for measurement of toughness in the polypropylene composites investigated. First there is the problem of accurate assessment of crack growth length. In particular, cracks observed in the PP/EPR sample were extremely small, making precise measurement very difficult. In the case of PP/G/EPR materials, the measurement of crack growth length was impossible, because, as indicated above, the deformation area consisted of many fine microcracks. Furthermore, the crack blunting line concept assumes a semicircular crack blunting profile ahead of the notch tip caused by plastic deformation and yielding. However, in the ternary phase PP composites studied, the crack tip does not appear to be blunted, but instead develops a rather complex damage zone resulting from a combination of local shear yielding, crazing and void formation (Fig. 8). The morphology of fracture surfaces and probable toughening mechanisms in these composites are discussed in more detail later.

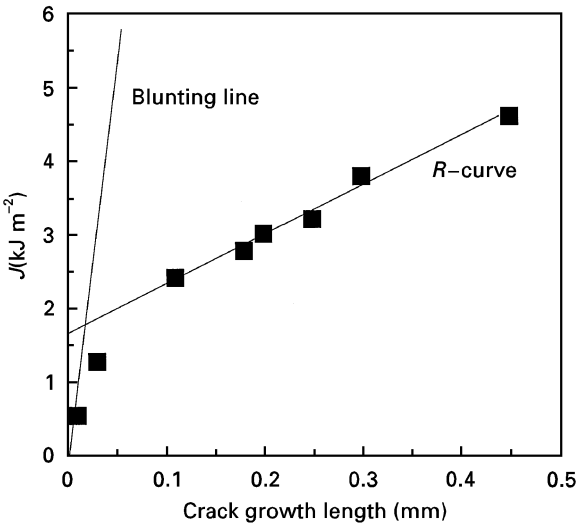

Figure 6 Plot of J against crack growth length for PP at $-20\,^{\circ}C$.

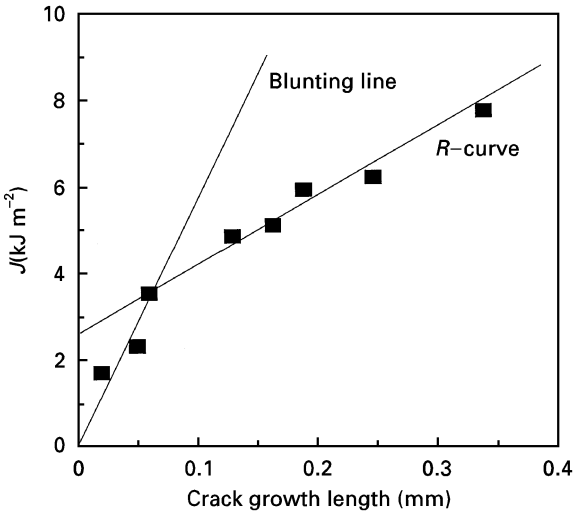

Figure 7 Plot of J against crack growth length for PP/EPR at $-20\,^{\circ}C$.

3.2. Toughness measurements using the stress-whitening zone method

At sufficiently high test loads, PP/elastomer compositions exhibited stress-whitening ahead of the initial notch, which progressively increased in size as the stress level was raised. Some workers [8, 10] have used the length of this whitening zone, instead of crack growth length, for the evaluation of J_c. Fig. 9 shows a typical load–displacement curve for PP/EPR specimens, where stress-whitening is seen to develop with increasing load (Fig. 9a–d). Calculated J-values for this blend are plotted against the stress-whitening length, Δl, in Fig. 10. It is evident that the resistance curve is formed from two lines of different slope. Initially, the stress-whitening length increased less rapidly with J, because applied energy is used only for the creation of crazes. Subsequently, the slope increases, as part of the energy input is consumed by crack growth, resulting in a retardation in the rate of stress-whitening. The intersection of these two lines is regarded as the onset of crack growth. Fig. 11 shows a plot of stress-whitening zone length, Δl, measured at the centre of the specimen against crack growth length, Δa, for the PP/EPR composition, where it is evident that the slope is higher in the earlier stages of deformation but decreases later. The intersection between these two lines is related to the crack initiation point.

From Fig. 10, a J_c value of $3.22\,kJ\,m^{-2}$ was obtained for PP/EPR measured by this method at

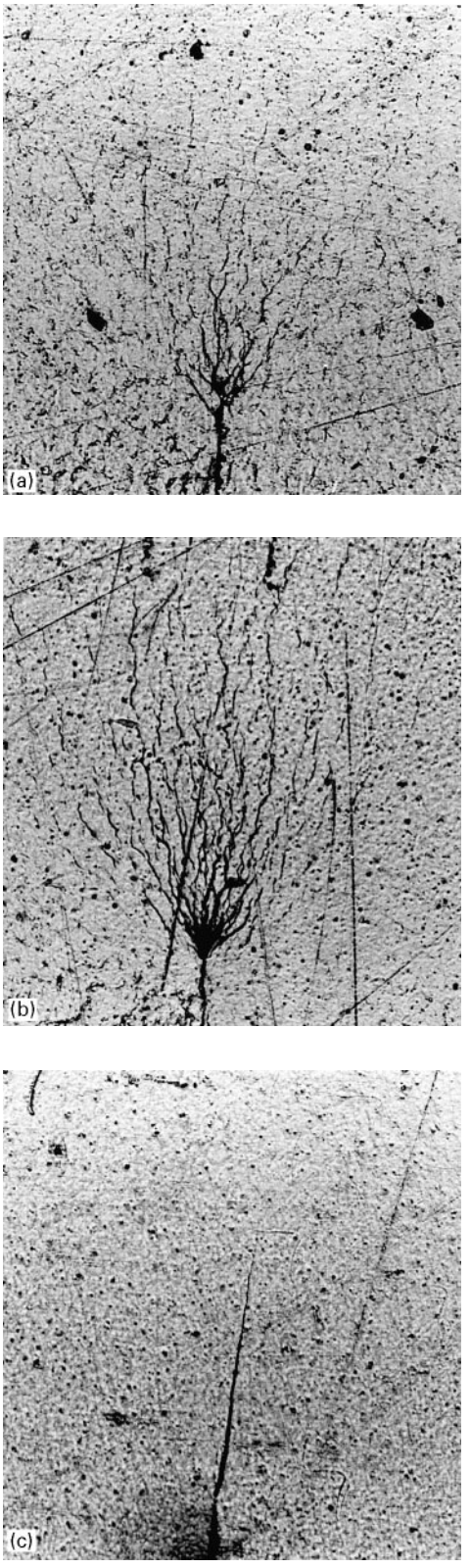

Figure 8 Optical micrographs of cracks observed on the surfaces of (a, b) PP/G/EPR and (c) PP.

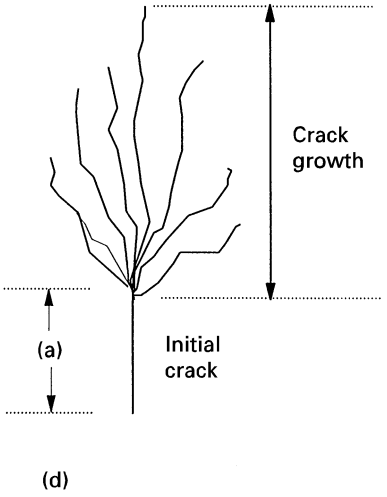

Figure 8 (Continued)

$-20\,^{\circ}C$, compared to 3.48 kJ m^{-2} using the conventional crack growth length approach (Fig. 7). Fig. 12 shows the relationship between J and stress-whitening length for the ternary phase PP/G/EPR composite, resulting in a J_c value of 0.82 kJ m^{-2}.

These results for PP/EPR composites demonstrate that at $-20\,^{\circ}C$. J_c values obtained by the stress-whitening technique are in good agreement with those from the more conventional approach. In addition, the stress-whitening method is also applicable to ternary phase PP/G/EPR composites, whereas where the conventional method is inappropriate due to the problem of determining a meaningful crack growth length. However, the method can be limited by the accuracy in assessing differences in slope of the two intersecting lines. In this context, Lee and Chang [10] characterized the fracture behaviour of elastomer-modified polycarbonates using the J integral procedure and found that the difference in slope decreased with increasing elastomer content.

Table I presents a summary of J_c values for various polypropylene composites obtained by the stress-whitening zone method at $-20\,^{\circ}C$, including compositions containing MaR. Incorporation of 30 vol % rubber into PP (either EPR or MaR), gave a significant increase in composite toughness. However, by using MaR instead of EPR, J_c was enhanced by more than 200%. In PP/G/EPR, inclusion of unfunctionalized rubber had little apparent effect on the reduction in toughness due to glass filler addition. However, incorporating MaR in place of EPR, greatly improved composite toughness to a higher value than for unmodified PP and to a similar level than for the PP/EPR binary blend, containing 30% by volume of rubber.

3.3. Observations on fracture surface morphology

Fig. 13 is a general view of a cryogenic fracture surface from a PP/EPR specimen showing three distinct zones. Zone I is the machined notch made by a band saw, zone II is the sharp notch introduced by the razor blade, and zone III is the surface morphology resulting from specimen fracture. At higher magnifications, further differences in morphology can be distinguished, proceeding from the notch tip towards the end of the fracture surface. The location of the features shown in Figs 14–18 for PP and different PP composites, is labelled as A–D in Fig. 13.

Fig. 14 shows fracture surfaces of a tested PP sample. At $-20\,^{\circ}C$, it is evident that PP exhibited predominantly brittle failure. Incorporation of EPR to PP, caused cavitation associated with extensive plastic deformation on the fracture surface (Fig. 15). Some

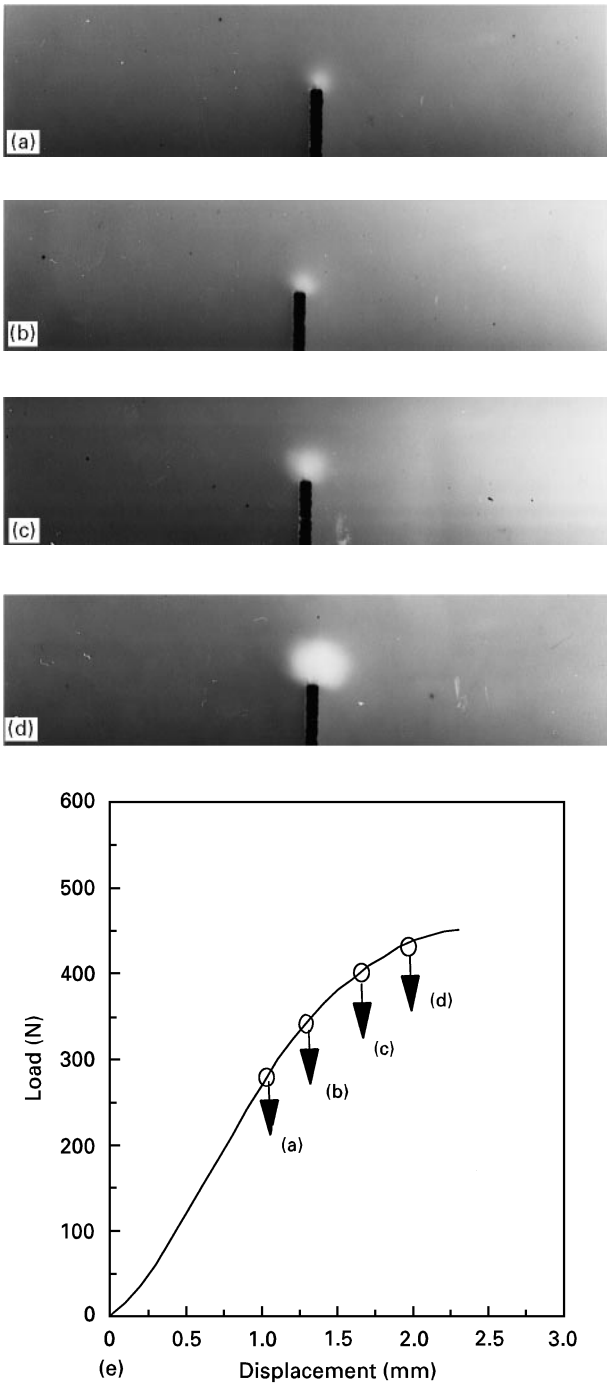

Figure 9 Development of stress-whitening zone in PP/EPR with increasing applied load.

cavitation is seen (Fig. 15a), which becomes more intense in the stress-whitening regime (Fig. 15b). Here, void diameters are much greater than the original rubber particle size (~ 1 μm). Some voids show evidence of coalescence and others are highly stretched and elongated, as the specimen deforms (Fig. 15c). The number of voids increases with strain until they eventually become interconnected, producing polypropylene fibrils lying parallel to the deformation direction (Fig. 15d). Ultimately, these fibrils break and fracture of the specimen ensures. The combined process of cavitation and shear yielding as toughening mechanisms in these PP/R blends, agrees well with the toughening mechanisms proposed for rubber-modified

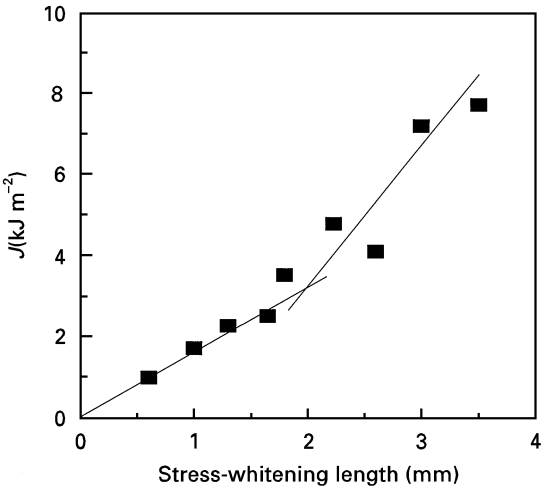

Figure 10 Plot of J against stress-whitening length for PP/EPR at $-20\,^{\circ}$C.

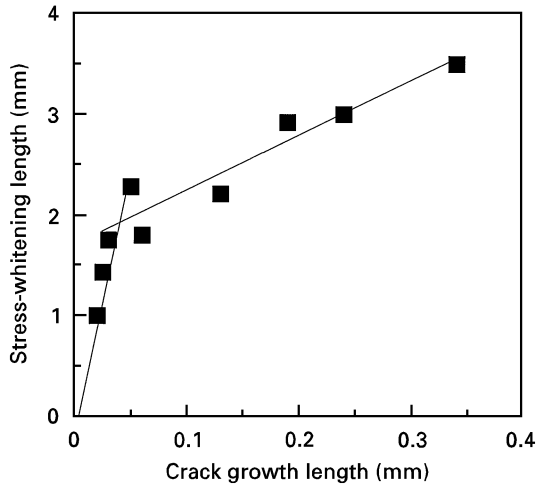

Figure 11 The relationship between stress-whitening length and crack growth length for PP/EPR at $-20\,^{\circ}$C.

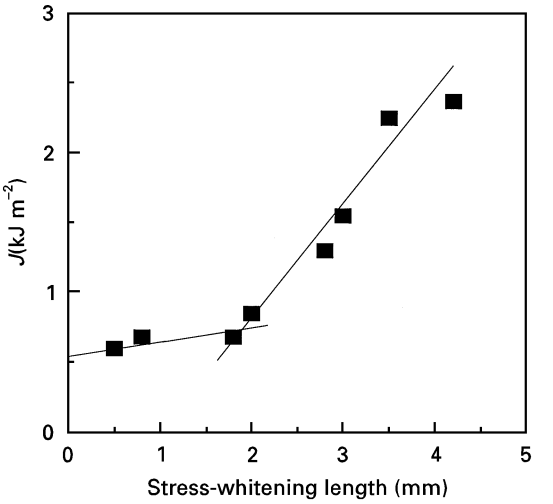

Figure 12 Plot of J against stress-whitening length for PP/G/EPR at $-20\,^{\circ}$C.

TABLE I J_c results for various polypropylene composites obtained by the stress-whitening method at $-20\,^{\circ}$C

Sample	Composition (vol %)	J_c (kJ m^{-2})	Yield stress (MN m^{-2})
PP	100	1.75[a]	51.8
PP/EPR	70/30	3.22	28.8
PP/MaR	70/30	6.13	25.5
PP/G/EPR	70/15/15	0.82	25.0
PP/G/MaR	70/15/15	3.33	20.1

[a] Measured using the crack growth method.

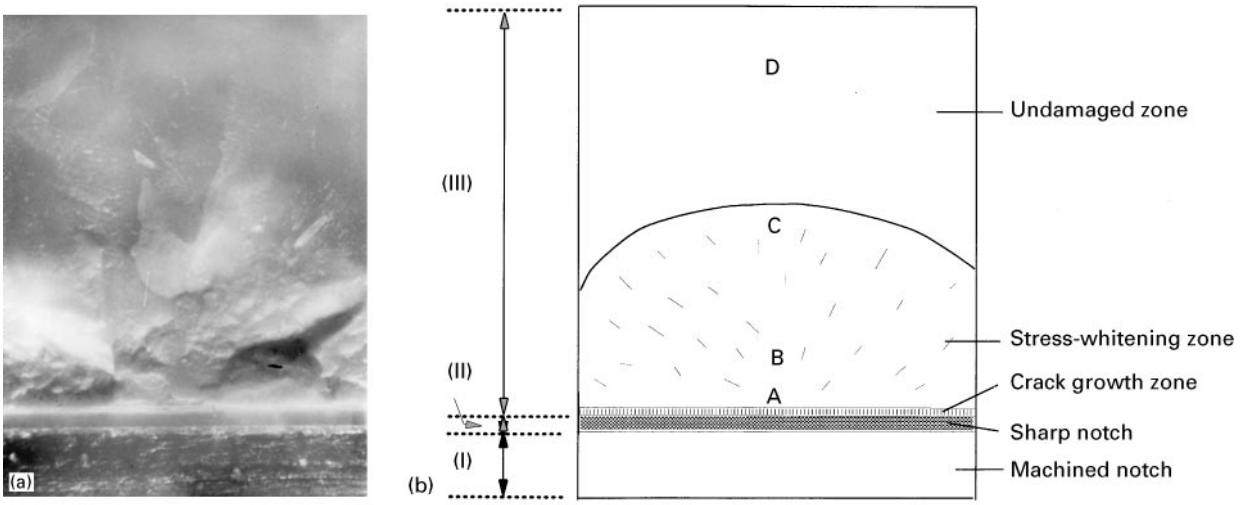

Figure 13 Typical fracture surface of J tested specimen showing three distinct zones: (I) machined notch, (II) sharp notch, and (III) fracture area.

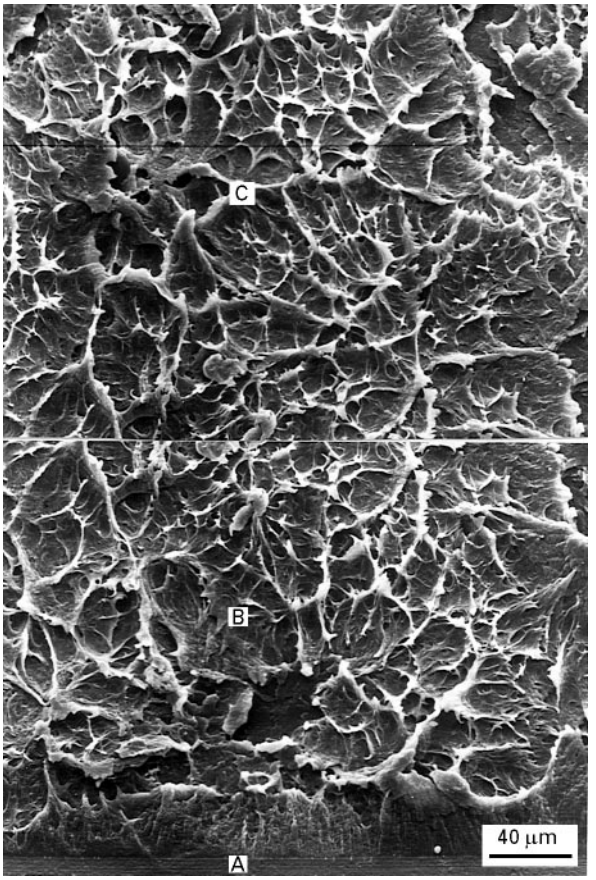

Figure 14 Scanning electron micrographs of crack-like features observed on the fracture surfaces of PP at $-20\,^{\circ}C$.

polyamide 6 [16, 17] and rubber-toughened polyamide 6,6 [18, 19].

Similar deformation behaviour was seen with the PP/MaR blend (Fig. 16). In addition to distinct rubber cavitation, some preferred alignment takes place suggesting the presence of shear bands. Haaf *et al.* [20] studied the deformation mechanism of rubber-modified PVC. They concluded that the dispersed rubber phase initiated micro-shear bands at an angle of 55°–64° to the direction of applied stress, depending upon the particle size of the modifier in the blend. Speroni *et al.* [21] also observed an angle of 76° between the directions of void stretching and void alignment in rubber-modified polyamide-6.

Figs 17 and 18 show fracture surfaces in ternary phase PP/G/EPR and PP/G/MaR compositions, tested at $-20\,^{\circ}C$. Crack propagation in the PP/G/EPR composite is consistent with particle–matrix debonding and pull-out, due to poor adhesion between glass bead particles and the polymer phases. However, the presence of MaR, in place of EPR, promotes adhesion

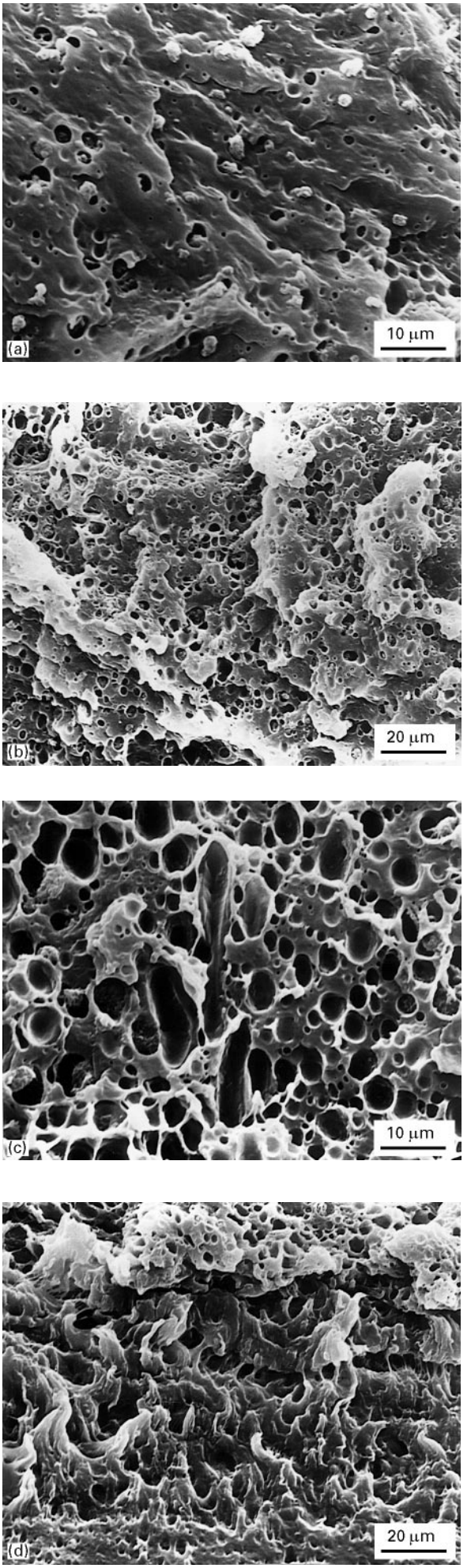

Figure 15 Ductile fracture surfaces of PP/EPR showing (a) cavitation and void formation, (b) greater cavitation density in stress-whitening zone area (B), (c) elongated voids in the areas B and C, and (d) PP shear yielding along the draw direction (area A).

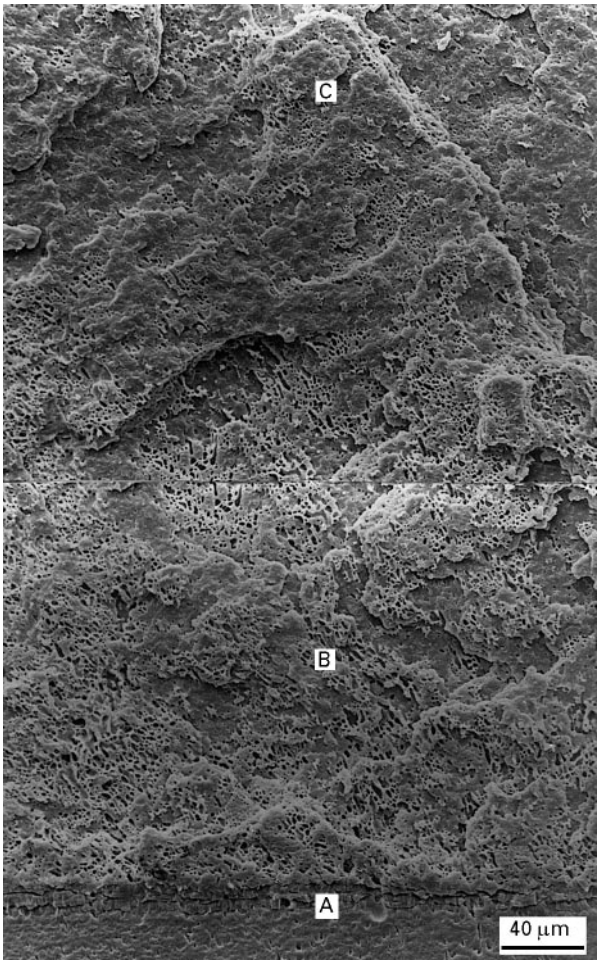

Figure 16 Fracture surfaces of PP/MaR (at − 20 °C) in areas A, B and C.

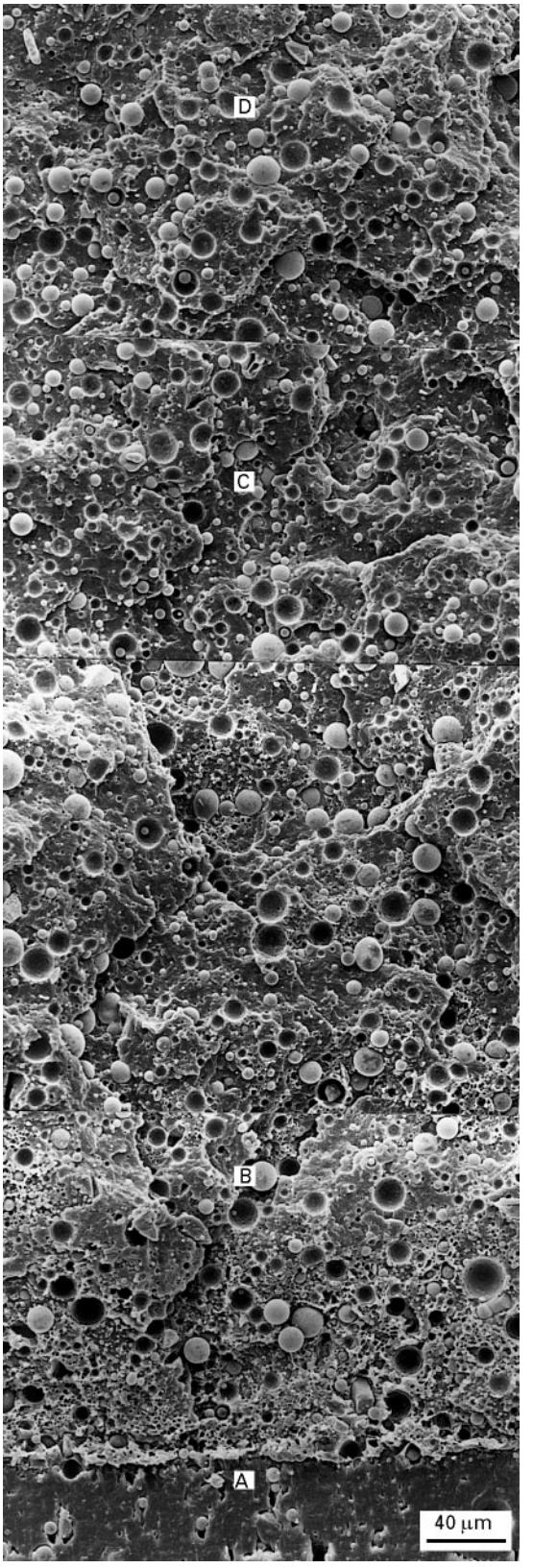

Figure 17 Fracture surface of PP/G/EPR (at − 20 °C).

to the glass filler, resulting in a markedly different topography. The fracture surface contains far fewer debonded glass particles and, in zone D, there is an indication that the crack has passed through the PP phase, causing cohesive failure. Scanning electron microscopy has also revealed evidence for rubber encapsulation around the filler in this system [22].

4. Conclusion

Two approaches have been investigated for determining J_c in multiphase PP composites. It was found that, at 23 °C, the crack blunting line approach can wrongly estimate J_c in rubber-modified polypropylene, and is unsuitable for the multiphase composites studied in this investigation, principally due to problems associated with accurate and meaningful measurement of crack growth length. However, by determining the length of the stress-whitening zone instead of the crack growth zone, a J value at crack initiation can be obtained. The toughness and failure mechanism of PP was found to change significantly by incorporation of EPR and glass beads. Scanning electron microscopy of fracture surfaces showed that crack growth arresting mechanisms involved cavitation, shear yielding and particle–matrix debonding. The presence of MaR in place of EPR dramatically changed the apparent failure mode, resulting in greatly reduced particle pull-out, and a significant enhancement in fracture toughness, in both binary and ternary phase systems.

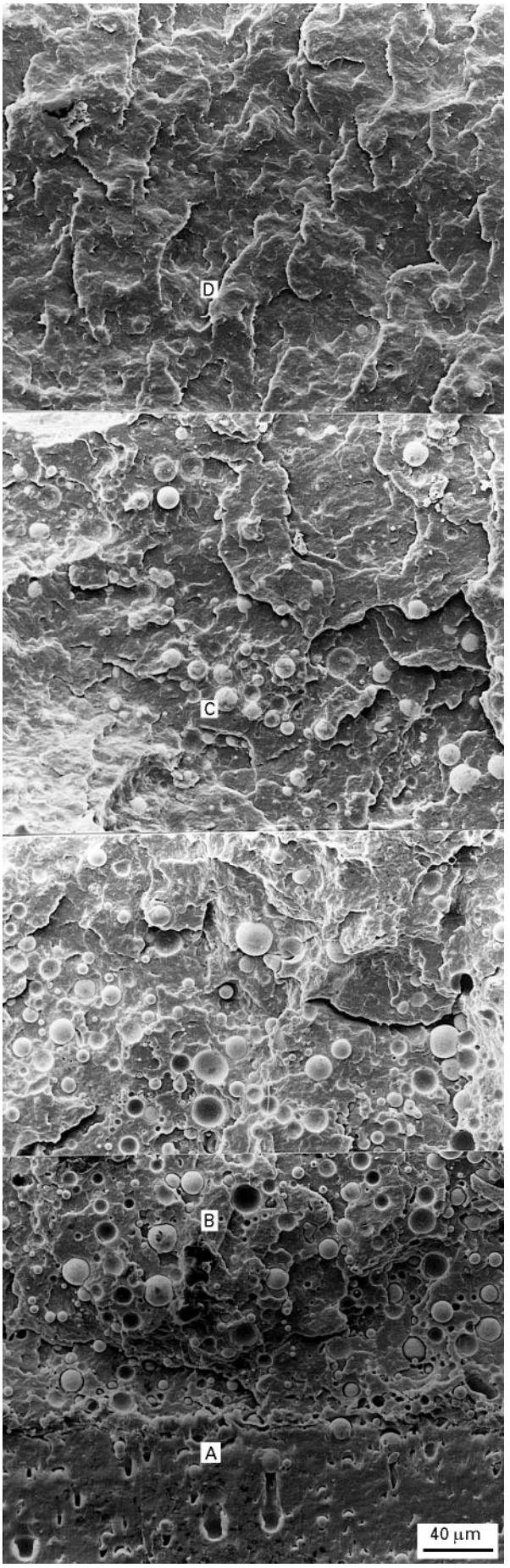

Figure 18 Fracture surfaces of PP/G/MaR (at $-20\,^{\circ}C$).

References

1. J. R. RICE, *J. Appl. Mech.* **35** (1968) 379.
2. ASTM standard E813-81 (American Society for Testing and Materials, Philadelphia, PA, 1982).
3. B. H. KIM, C. R. JOE, and D. M. OTTERSON, *Polym. Testing* **8** (1989) 119.
4. I. NARISAWA, *Polym. Engng Sci.* **27** (1987) 41.
5. S. HASHIMI and J. G. WILLIAMS, *ibid.* **26** (1986) 760.
6. *Idem*, *Plas. Rubb. Proc. Appl.* **6** (1986) 363.
7. *Idem*, *Polymer* **27** (1986) 384.
8. M-J. ZHANG, F-X. ZHI and X-R. SU, *Polym. Engng Sci.* **29** (1989) 1142.
9. D. D. HUANG and J. G. WILLIAMS, *J. Mater. Sci.* **22** (1987) 2503.
10. C. B. LEE and F. C. CHANG, *Polym. Engng Sci.* **32** (1992) 792.
11. I. NARISAWA and M. T. TAKEMORI, *ibid.* **29** (1989) 671.
12. C. HA, Y. KIM and W. CHO, *J. Polym. Sci.* **51** (1994) 1381.
13. B. H. KIM and C. R. JOE, *Polym. Testing* **7** (1987) 355.
14. *Idem*, *Engng Fract. Mech.* **32** (1989) 225.
15. *Idem*, *ibid.* **32** (1989) 155.
16. R. J. M. BORGGREVE, R. J. GAYMANS, J. SCHUIJER and J. F. INGEN HOUSZ, *Polymer* **28** (1987) 1489.
17. S. WU, *ibid.* **26** (1985) 1855.
18. F. RAMSTEINER and W. HECKMANN, *Polym. Commun.* **26** (1985) 199.
19. C. B. BUCKNALL, P. S. HEATHER and A. LAZZEU, *J. Mater. Sci.* **16** (1989) 2255.
20. F. HAAF, H. BREUER and J. STABENOW, *J. Macromol. Sci. Phys.* **B14** (1977) 387.
21. F. SPERONI, E. CASTOLDI, P. FABBRI and T. CASIRAGHI, *J. Mater. Sci.* **24** (1989) 2165.
22. K. PREMPHET, PhD thesis, Brunel University, UK (1995).

Received 23 September 1996
and accepted 4 April 1997